The Canadian Mineralogist
Vol. 33, pp. 333-347 (1995)

AN SEM ELECTRON-CHANNELING STUDY OF FLAME PERTHITE FROM THE KILLARNEY GRANITE, SOUTHWESTERN GRENVILLE FRONT, ONTARIO

LYNN L. PRYER* AND PIERRE-YVES F. ROBIN
Department of Geology, Erindale College, University of Toronto, Mississauga, Ontario L5L 1C6

GEOFFREY E. LLOYD
Department of Earth Sciences, The University, Leeds LS2 9JT, U.K.

ABSTRACT

Flame perthite from greenschist-facies mylonites in the Killarney granite, near Georgian Bay, in Ontario, have been examined using SEM back-scattered-electron (BSE) images and electron-channeling patterns (ECPs). ECPs provide complete crystallographic orientation of a grain, or a part of a grain, as small as 5 μm, and can be done anywhere within a polished section. Also, EC involves high-resolution BSE imaging, and can distinguish phases on the basis of mean atomic number rather than optical properties; it is therefore particularly useful in studying feldspars. Using ECPs and BSE images, we determined (1) the relative crystallographic orientation of the host with respect to the flame, (2) the preferred growth-plane of the flames within the structure of the host K-feldspar, and (3) the orientation of the flames relative to the strain fabric in the host rock. This method gives more complete and more accurate information than the U-stage, and provides spatial information that cannot be obtained with X-ray-diffraction texture analysis. The K-feldspar host and the albite flames share the same crystallographic orientation. The dominant plane along which flame growth has occurred within the K-feldspar structure is the same as that for perthite of exsolution origin (*i.e.*, parallel to the *b* axis and approximately 9° from the *c* axis). Only in cases where multiple sets of flames are developed within a single crystal do other orientations occur. Relative to the rock fabric, flames are preferrentially oriented within a range subnormal to the *C* and *S* foliations; where two feldspar grains come in contact, flames also develop normal to their contact boundaries. Therefore, K-feldspar grains that are crystallographically oriented with the perthite plane subparallel to the local maximum stress direction exhibit growth of abundant flames. Grains in other orientations develop only minor flames or none at all.

Keywords: electron channeling, scanning electron microscopy, flame perthite, feldspar, crystallographic orientation, Killarney granite, Ontario.

SOMMAIRE

Une intercroissance perthitique en flammes provenant de mylonites déformées lors d'un métamorphisme au facies schistes verts dans la granite de Killarney, près de la baie Georgian, en Ontario, a été examinée au microscope électronique à balayage avec clichés par rétrodiffusion d'électrons (RDE) et clichés de schémas de canalisation d'électrons (SCE). Les clichés SCE donnent l'orientation complète de grains, ou de portions de grains, de taille 5 μm ou plus, et peuvent être obtenus en tout point de la surface d'une section polie. Leur collecte est en outre associée à des clichés RDE de haute résolution qui permettent de distinguer les phases grâce à leurs nombres atomiques moyens plutôt qu'à leurs propriétés optiques; la méthode est donc particulièrement utile pour l'étude des feldspaths. L'étude a permis de déterminer l'orientation préférentielle des flammes albitiques (1) par rapport aux axes de fabrique de la roche et (2) par rapport au réseau cristallin de leur hôte potassique, ainsi que l'orientation cristallographique de l'albite. Cette méthode d'analyse de textures fournit une information plus complète et plus précise qu'avec la platine universelle sous microscope optique, et permet aussi une localisation de chaque analyse qui serait impossible par les méthodes utilisant les rayons X. Les flammes albitiques et leur hôte potassique partagent la même orientation cristallographique. Les flammes sont majoritairement parallèles au même plan que les lamelles perthitiques d'exsolution, c'est-à-dire, parallèles à l'axe *b* et faisant un angle d'environ 9° avec l'axe *c*. Des flammes ayant des orientations autres que celle des perthites d'exsolution ne sont observées que lorsque plusieurs groupes de lamelles perthitiques coexistent dans un même grain. Les flammes sont en majorité soit normales à la foliation *S* de la roche, soit perpendiculaires à la surface de contact entre deux grains adjacents; elles sont donc interprétées comme étant parallèles à une direction de compression maximale. Les grains de feldspath potassique dont les réseaux cristallins n'ont pas la bonne orientation par rapport à ces contraintes extérieures ne montrent que des flammes mineures ou même pas du tout.

Mots-clés: canalisation d'électrons, microscopie électronique à balayage, perthite en flammes, feldspath, orientation cristallographique, granite de Killarney, Ontario.

---

*Present address: Research School of Earth Sciences, Australian National University, Canberra 0200, Australia.

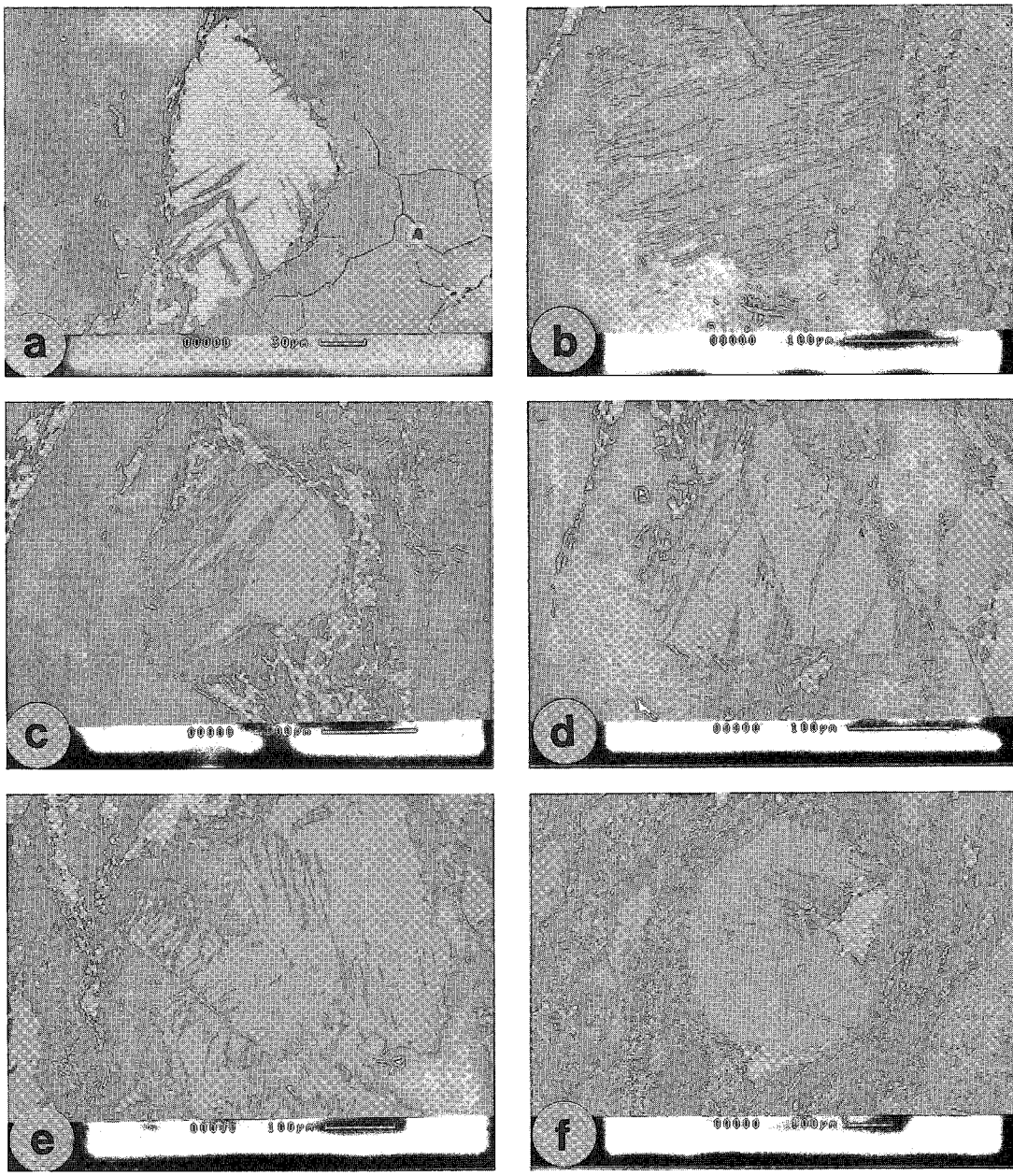

FIG. 1. Back-scattered electron images of some of the grains of flame perthite used to collect electron-channeling patterns (ECP) of host and lamellae. All flames follow the preferred orientation for perthite lamellae except in grains where more than one set is developed. (a) P231, grain 113: two sets of flames are developed. The set trending from the top right to bottom left has the perthite orientation; the other set is near the (001) cleavage. Both sets and host are homotactic. Orientation contrast (OC) can be seen in the surrounding quartz matrix. (b) Grain 117 shows approximately 40% replacement. Flames are wider at grain boundaries and fractures. (c) Grain 118 shows heterogeneous replacement (30–40%). The quartz ribbon to the left of the grain shows OC. The small grain of perthite, above right of grain 118, shows 70–80% replacement. (d) Flame perthite in an albite matrix; internal flames initiate along a central fracture in the grain. (e) Grain 120, two sets of flames; the set trending *ca.* 25° counter-clockwise from the vertical are very thin and straight and have the perthite orientation. The other set is more sigmoidal and shorter, originating from a microfault. (f) P139, grain 003; flame perthite grain in a strongly foliated matrix. The prominent foliation is the *C* plane. Note the abundant small grains of flame perthite in the matrix.

Introduction

Electron channeling (EC) is a consequence of the diffraction of electrons by the structure of a crystal. In a scanning electron microscope (SEM) operated in back-scattered electron (BSE) mode, an electron-channeling pattern (ECP) can be produced to provide complete information on the crystallographic orientation of the target crystal. ECPs are the BSE equivalents, in scanning electron microscopy, to Kikuchi patterns observed in transmission electron microscopy. Since independent ECPs can be obtained at intervals of 10 μm over an entire polished section, they are a powerful tool to characterize orientation relationships of minerals and mineral intergrowths in rocks. After a brief review of the theory of electron channeling and the methodology of producing and analyzing ECPs, we present their application to the characterization of flame perthite in the Killarney granite, southwestern Grenville Province, in Ontario. Specifically, we determined (1) the orientation of the K-feldspar relative to the host-rock microstructure, (2) the orientation relationship between the albite flames and the K-feldspar host, and (3) the orientation of the flames relative to the host-rock fabric, using a single technique.

Flame Perthite

Flame perthite consists of intergrowths of flame-shaped albite lamellae in a K-feldspar host crystal. It occurs in mylonite developed during retrograde greenschist-facies metamorphism. Flame perthite forms when Na replaces K in K-feldspar. The Na is released by the retrograde reaction of plagioclase, in which the anorthite component reacts with the limited water available to form epidote. The K replaced by the Na migrates back to the altering plagioclase to produce muscovite (Pryer 1993b).

The flame-shaped lamellae occur in distinct sets of single or multiple parallel flames within K-feldspar grains. Most commonly, flames originate at grain boundaries or at fractures within grains (*e.g.*, Figs. 1i, j) and taper to a point within the grain. They may also occur completely within the host grain, at least as seen in section, or at inferred points of high stress such as at the contact between feldspar grains. Within a typical sample of quartzofeldspathic mylonite, some K-feldspar grains may show as much as 50% replacement by albite flames, whereas others show no evidence of replacement.

Flames seem to have a preferred orientation relative to the rock fabric. Finite tectonic strain in a rock is characterized by its *X*, *Y*, and *Z* directions. *X* is the direction interpreted to be that of maximum principal tectonic strain; *Y* is parallel to the foliation and perpendicular to *X*; *Z* is normal to both *X* and *Y* and, for all intents and purposes, is normal to the main foliation. A monoclinic rock-fabric is commonly developed in mylonite; it is expressed in the rocks studied here by a S–C fabric (Fig. 2; Berthé *et al.* 1979, Lister & Snoke 1984). In thin sections cut parallel to the *XZ* plane, the long dimension of the flames in grains of flame perthite has a preferred orientation relative to the *S–C* fabric in the mylonite, subnormal to the S foliation (Fig. 3).

The variability in extent of replacement and the preferred orientation of the flames relative to the fabric of the host rock indicate that there may be a crystallographic control on orientation of the flames. In order to address the problem of orientation control, it is necessary to characterize (1) the preferred orientation of the albite flames relative to the rock fabric, (2) the crystallographic orientation of the flames relative to the host K-feldspar, and (3) the crystallographic orientation of the host K-feldspar relative to the rock fabric. We contend that all of these relationships can be shown most easily by the use of a single technique: electron channeling on the scanning electron microscope.

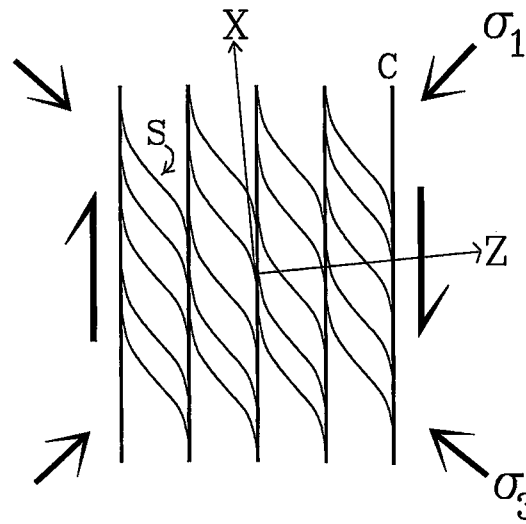

FIG. 2. Sketch of *S* and *C* foliations showing the symmetry of the microstructural fabric and the inferred stress-directions in a *S–C* fabric: σ_1 and σ_3 are the maximum and minimum principal compressive stresses, respectively. The direction of intermediate principal strain, *Y*, which is also the 2-fold axis of symmetry of the monoclinic fabric, is normal to the plane of the sketch. The direction of maximum principal extension, *X*, is inferred to be within the acute angle between the *S* and the *C* directions. The direction of principal shortening, *Z*, is normal to *X* and *Y*. The sense of shear along the *C* plane is shown.

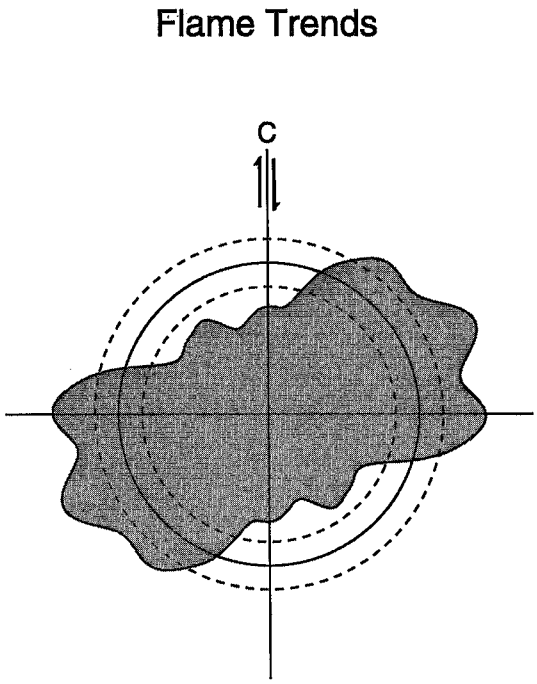

FIG. 3. Two-dimensional distribution of the orientation of the long axes of 3222 flames measured in the *XZ* section. The diagram is in the same orientation as Figure 2. The solid circle gives the expected (average) value, *E*, of the orientation density. The dashed circles correspond to departures from *E* that are considered significant. Flames have a strong preferred orientation normal to the *S* foliation in the host rock.

CRYSTALLOGRAPHIC ORIENTATION ANALYSIS WITH ELECTRON CHANNELING

Electron channeling (EC) was first observed in the SEM by Coates (1967) and is well established in metallurgy and material sciences (Joy *et al.* 1982, Newbury *et al.* 1986). SEM–EC techniques have remained in relatively minor usage in the earth sciences because few SEM designs have been capable of the overall perfomance required for serious crystallographic investigations.

Electron channeling

The intensity of a BSE signal is mostly determined by the mean atomic number of the target. However, EC is responsible for small (< 5%) but significant variations in the BSE signal. Incident electrons are channeled by atomic planes *via* coherent Bragg scattering of the inelastically scattered electrons (Fig. 4). Thus,

FIG. 4. Electron-channeling effect. When the incident electron beam strikes a given lattice plane, (*hkl*), at the Bragg angles, θ_B, as in (a) and (c), electrons are channeled as a result of coherent scattering, and a lesser fraction is scattered back to the detector. When the electron beam strikes the lattice plane at less than θ_B, as in (b), a greater fraction of the incident beam is back-scattered. In a BSE image produced by rocking or scanning the beam, the lattice plane gives rise to a bright band with a width of $2\theta_B$. Kikuchi patterns observed in the TEM are negatives of ECPs.

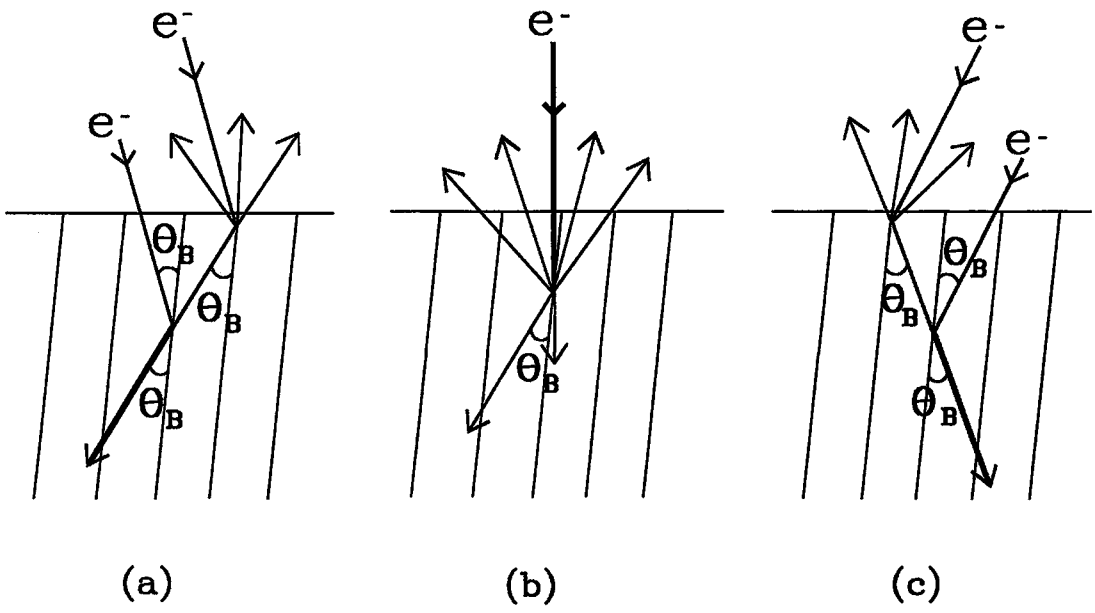

the probability of channeling depends on the angle between the beam of incident electrons and the various planes of atoms. For a particular set of planes, (*hkl*), the most significant changes in the probability of channeling (and hence in the magnitude of the EC portion of the BSE signal) occur about integer values of the Bragg diffraction angle (θ_B). Because the extent of interaction between electrons and crystal structure depends on the angle of beam incidence, characteristic changes in BSE–EC emission only occur when all electrons are traveling in the same direction; therefore, observation of EC requires a well-collimated beam (*i.e.*, divergence angles $<10^{-3}$ radian).

Orientation contrast and electron-channeling patterns

The EC effect can be recognized and studied with two types of images: *orientation contrast* (OC), also known as *crystallographic* or *channeling contrast*, and ECPs. An OC image is seen in regular scanning mode; it is well illustrated in the quartz grains surrounding the flame perthite in Figure 1c, where individual grains and subgrains can be distinguished. The contrast between grains is determined by differences in their respective amounts of channeling, which in turn is a function of their crystallographic orientations relative to the beam. However, it does not reflect the magnitude of the misorientation between individual regions.

To produce a useful ECP, the incident angle of the beam must be varied by an angle of ~20°, and the BSE intensity measured as a function of orientation. An ECP is thus obtained either by rastering on a large grain or by rocking the electron beam about a fixed point. In the latter case, the rocking angle is determined by the angle the incident beam subtends with the target, which requires that the working distance, (*i.e.*, the distance between the lower aperture and the sample) be less than 10 mm. In addition to the small working-distance, high contrast and a large black-level correction are needed to produce a channeling pattern. The necessary modifications to the normal operating conditions in the SEM (Fig. 5) are discussed in detail by Lloyd (1985, 1987).

An ECP consists of a unique configuration of contrast lines or bands (*e.g.*, Fig. 6c), each of which represents a specific EC interaction with a particular set of crystal planes. Therefore, the whole pattern defines the crystallographic orientation at the point of incidence. Lateral movement of the specimen does not alter the appearance of the ECP unless the crystallographic orientation changes (*e.g.*, the beam crosses a grain or subgrain boundary), because the angular relationships between incident beam and crystal planes

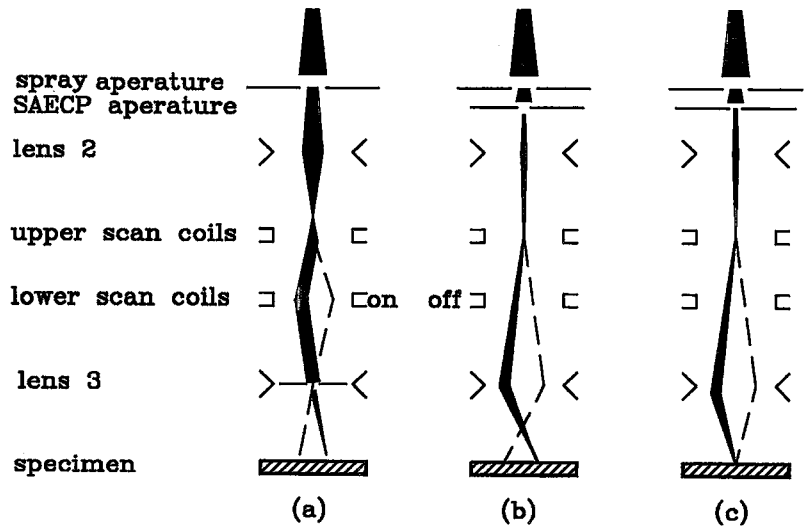

FIG. 5. Schematic ray-diagram for SEM operation in (a) normal, and (c) selected-area ECP mode. When the cross-over point of the beam is above, as in (b), or below the sample, the image produced is a combination of BSE and ECP images (Fig. 6b) (after Lloyd *et al.* 1981, Newbury *et al.* 1986).

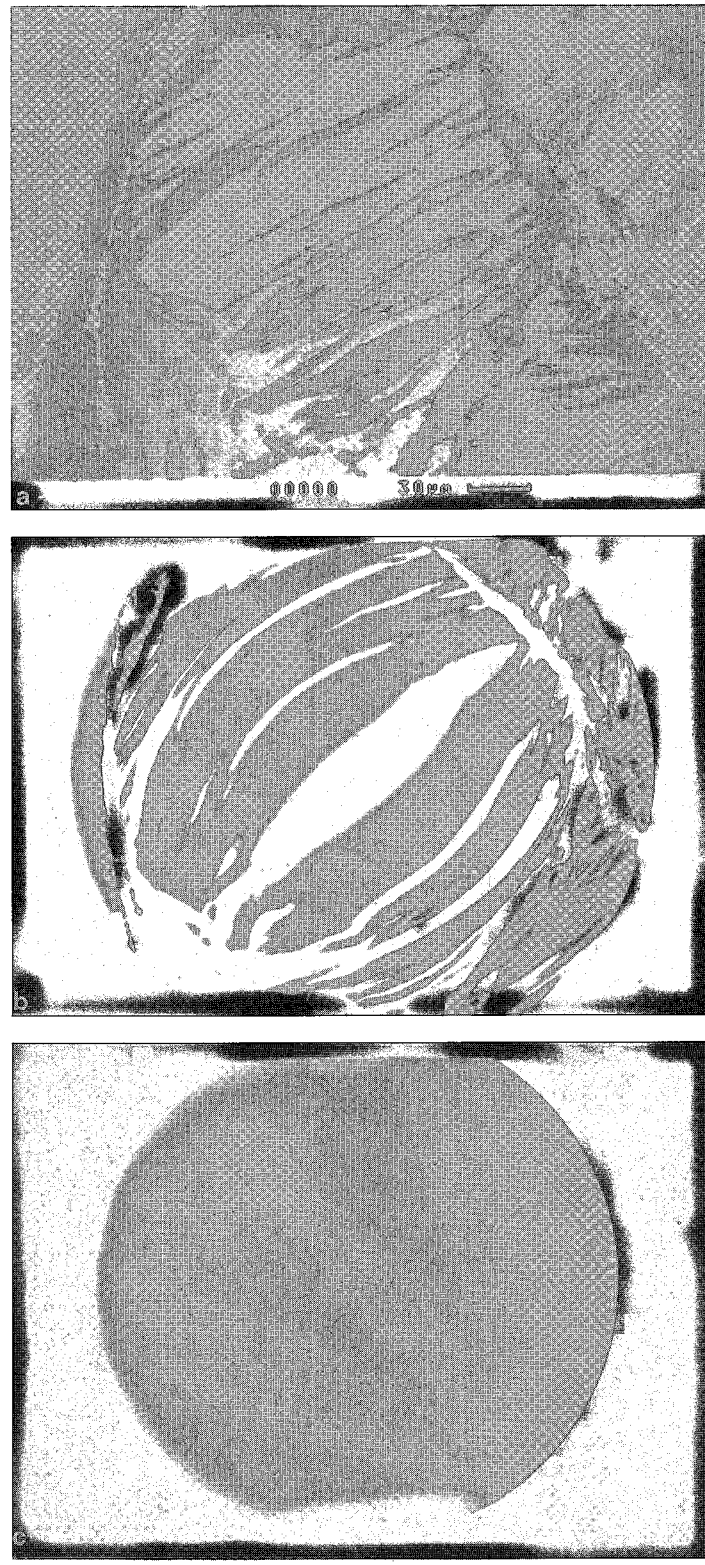

FIG. 6. A good illustration of the effect on the BSE image as the cross-over point of the electron beam is lowered to the surface of grain 116. (a) Normal BSE image with beam scanning as in Figure 5a. K-feldspar is grey, albite is black. (b) Cross-over point half way between its scanning and rocking positions, as in Figure 5b. Note the continuity of the channeling pattern within the K-feldspar host, uninterrupted by the albite lamellae. (c) ECP produced when the cross-over point is at the specimen surface, as in Figure 5c.

remain constant. However, tilting the specimen will change the ECP, as the relative orientation of the crystal structure changes with respect to the incident beam. Preferably, ECPs are collected on specimens positioned normal to the incident beam of electrons.

Figure 6a shows a BSE image of a grain of flame perthite produced in scanning mode with a working distance of 5 mm. To change the image from OC mode to ECP mode requires some modification to the lenses and apertures within the electron column (Fig. 5b). Figure 6b shows the resulting image once this switch is made, but the focal point (cross-over point) of the rocking beam is not positioned on the surface of the sample. As the cross-over point is brought to the specimen's surface, the area from which the ECP is collected is reduced to a single spot (Figs. 5c, 6c). However, note that the ECP in Figure 6c can be seen clearly throughout the entire grain imaged in Figure 6b, uninterupted by the albite flames (black areas).

Effects of sample deformation

The spatial and angular resolutions achieved depend not only on the beam conditions, but also on the nature of the specimen, particularly if the specimen is deformed. Specimens must have a constant lattice-orientation over the region about which the beam is rocked in order to produce a good pattern. "Hot-working" and "cold-working" of crystals, resulting from deformation, will have an effect on the ECP produced. "Cold-working" refers to the presence in the crystal of a large density of dispersed dislocations resulting from relatively low-temperature or high-strain-rate deformation, and includes the effects of specimen preparation; it results in a loss of fine detail and contrast. "Hot-working" refers to a dislocation structure indicative of recovery; it results in distortion of the ECP (*i.e.*, bending and irregular band-widths) due to the development of subgrains with slightly different orientations. If indistinct ECPs are observed, they are normally attributed to hot or cold working, and the grain must be moved under the electron beam until an indexable ECP is obtained.

Comparison of ECP with other techniques

(1) The *petrographic microscope equipped with a Universal stage* only gives the orientation of the optical indicatrix, which must then be transformed into crystallographic directions. As the orientation of the indicatrix can change with the degree of Al–Si order and composition, this process can be tedious. For the orientation of triclinic minerals, the U-stage also requires that the orientation of at least one crystallographic feature, such as a cleavage or twin plane, be known. EC is more accurate and more rapid (especially for low-symmetry minerals), and allows the complete determination of the crystallographic orientation of most minerals. Another advantage over the U-stage is that SEM–EC has a resolution on the order of 10 μm, far better than the petrographic microscope. In this study, it has been possible to determine the orientation of thin lamellae of albite that, on the U-stage, would effectively disappear as the stage is tilted.

(2) In *X-ray fabric analysis*, overlapping 2θ peaks are a major problem for triclinic minerals such as feldspars. Also, this technique in general requires that phases or grain populations that are not of interest be removed from the section, whereas SEM–EC can be done on samples with mixed phases (*e.g.*, quartz and feldspar) or mixed grain-sizes.

(3) *Laue microdiffraction* and other *single-crystal X-ray methods* may be capable of determining the crystallographic relationship between host and flame, but in EC, the same information can be obtained while easily maintaining spatial information, as samples are examined as intact polished specimens rather than as separated grains.

(4) *Transmission Electron Microscopy (TEM)* only allows examination of very small areas, and is therefore impractical for bulk-fabric analysis. Sample preparation for SEM–EC is more straightforward than for TEM. The area that can be examined in the SEM is limited only by the size of the sample holder. EC thus allows examination of an entire polished section.

(5) *Electron Back-Scatter Diffraction (EBSD)* also relies on the phenomenon of electron channeling but differs from the EC method used here in that the electron beam is stationary. The change in angle needed to produce the diffraction pattern is achieved by detecting over an angular range rather than rocking the incident beam. This requires that the sample stage be tilted at a moderate angle to the incident beam, in order to accommodate the EBSD detector. Although EBSD is capable of much higher resolution, BSE examination of the area to be analyzed by EBSD requires constant adjustment of sample position and orientation. ECP collection does not require that the sample be tilted relative to the electron beam, and it is possible to image grains in orientation-contrast mode and collect ECPs without changing the orientation of the sample.

It should also be noted that ECP analysis is typically combined with the production of a high-resolution BSE map of the sample. A beneficial consequence of the extra preparation necessary for EC is the orientation contrast which, unlike standard BSE analysis, permits the distinction of individual grains and subgrains of the same mineral.

Experimental Procedure

The samples used in this study are taken from the Killarney granite, which outcrops 20 km north of Georgian Bay on the southwestern Grenville Front, in Ontario (Pryer 1993a, Haggart *et al.* 1993). Two samples were cut from mylonite, which formed during

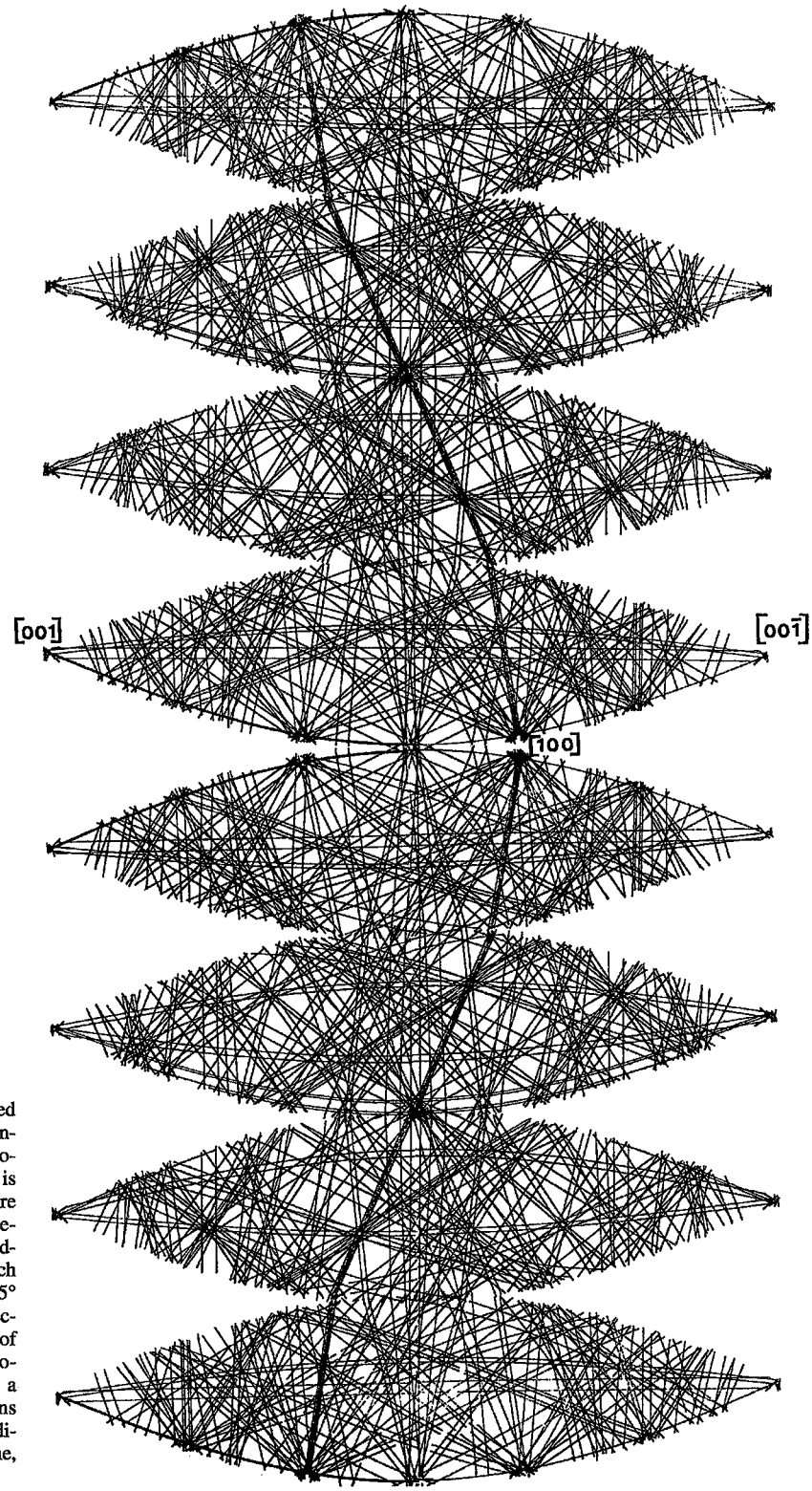

FIG. 7. Computer-generated map of the electron channeling bands for microcline. A lattice plane is represented by 1 or more pair(s) of lines corresponding to the boundaries of the band. Each segment represents a 45° section of the total reflection-sphere. The tips of each segment join together to produce a sphere. The directions [100] and [001] are indicated, and the basal plane, (001), is shaded.

thrust faulting and have undergone retrograde metamorphism to the greenschist grade. Extensive electron-microprobe analyses have been done on the feldspars from this area and show their compositions to be very consistent both within a sample and from one sample to the next (Pryer 1993b). The mean composition of K-feldspar in all samples that contain flame perthite is 94.55 ± 1.15% Or; whereas that of albite in all flames and matrix grains is 97.55 ± 0.72% Ab. BSE and EC analyses were done at Leeds University on a CAMSCAN (Cambridge Instruments) Series 4 SEM incorporating a dynamic Selected Area Diffraction (SAD) attachment and a KE Electronics 4-quadrant, solid-state BSE detector.

In the preparation of polished thin-sections, the surface topography is normally removed by successively finer grades of carborundum or diamond abrasives. However, this procedure leaves a severely damaged surface-layer, called the Bilby layer, and must be removed for electron channeling to be observed. This can be done by chemical or electrochemical polishing, or by a combination chemical and mechanical polishing agent used with a standard polishing machine. Details of sample preparation are described by Lloyd (1985) and Lloyd *et al.* (1981).

Indexing of ECPs

Until recently, in order to index patterns of unknown orientation, it was necessary to use spherical maps of collected ECP images (*e.g.*, Lloyd & Ferguson 1986) or computer-drawn maps and a visual search to locate the position of the unknown ECP. Computer-drawn maps (*e.g.*, Fig. 7) show only band edges and give no information on intensity, which makes it difficult to compare the ECP image from the SEM with the map. SEM–ECP can now be indexed by the computer. In this study, the software CHANNEL© (Schmidt & Olesen 1989) has been used; it requires inputs of 1) the Laue group of the mineral, and 2) the atomic species and their positions. The computer-generated map resides in memory along with the intensity information. The patterns are indexed by digitizing two or more bands, using a video print on a digitizing tablet, or digitizing directly on the computer screen using a video image collected from the SEM. Each ECP band is transformed by the computer into a lattice plane with a *d*-value calculated from the band width. The computer searches the calculated ECP map for a match, and the area selected is shown on the computer monitor. The match can then be examined before it is accepted. Symmetry dictates the proportion of the reflection sphere necessary for indexing and, therefore, the size of the map that must be searched for indexing; the triclinic symmetry of feldspars means that the entire sphere of reflections must be considered.

Under normal OC mode, a BSE map of the entire sample was collected. In sample P231, ECPs were collected from 120 K-feldspar grains from which a recognizable pattern could be derived; 49 of the collected K-feldspar patterns (41%) could be indexed using CHANNEL©. Perthite grains were selected from the BSE map, and ECP were collected for 10 host–flame sets in sample P231 and five pairs in sample P139 using the best-developed flames from each grain. Flames must be wider than 10 μm to give a good pattern that fills the entire field of view. The host K-feldspar from the perthitic grains was indexed as microcline (Blasi *et al.* 1984), and flame albite was indexed as high albite (Prewitt *et al.* 1976). The reason for indexing as high rather than low albite will be discussed below.

RESULTS

Preferred orientation of K-feldspar relative to the rock fabric

Based on the grains indexed (which represent 41% of the feldspar grains with good ECPs), there is a weak preferred orientation of crystallographic axes (Fig. 8). The interdependence of the fabrics is clearly illustrated in Figure 8; the *a*-axis maximum is normal to the *b*-axis girdle, and the *c*-axis girdle trends through the gap in the *b*-axis girdle. The obliquity of these patterns to the *XZ* section may indicate that either the rock fabric is triclinic or the section was not cut exactly normal to the local *Y* direction.

It is important to note, however, that these data may not be a representative sample of the feldspar population. Because of cold-working in many of the grains, a 1-cm^2 section produced good ECPs from only 120 grains larger than 100 μm. Of these, only 49 patterns could be indexed. Since some orientations are easier for CHANNEL to identify than others, there may be a bias in the 41% of the patterns that could be indexed. The problems with indexing feldspar ECPs, discussed below, need to be addressed before a more detailed analysis of the feldspar fabrics can be done (*e.g.*, separating populations of different grain-sizes and morphologies).

Determination of preferred orientation of the flames

The trends of the flames were measured in sections cut parallel to the lineation (*X* direction) and perpendicular to the foliation (*Z* direction) using photomicrographs from the BSE image map. The length and orientation of each flame in sample P231 were digitized by hand on a SummaGraphics digitizing tablet and compiled; they show that there is a preferred orientation of flames relative to the *S–C* fabric (Fig. 3). Flames tend to form with their long axes normal to S-foliation, and therefore parallel to the inferred direction of maximum compression (σ_1).

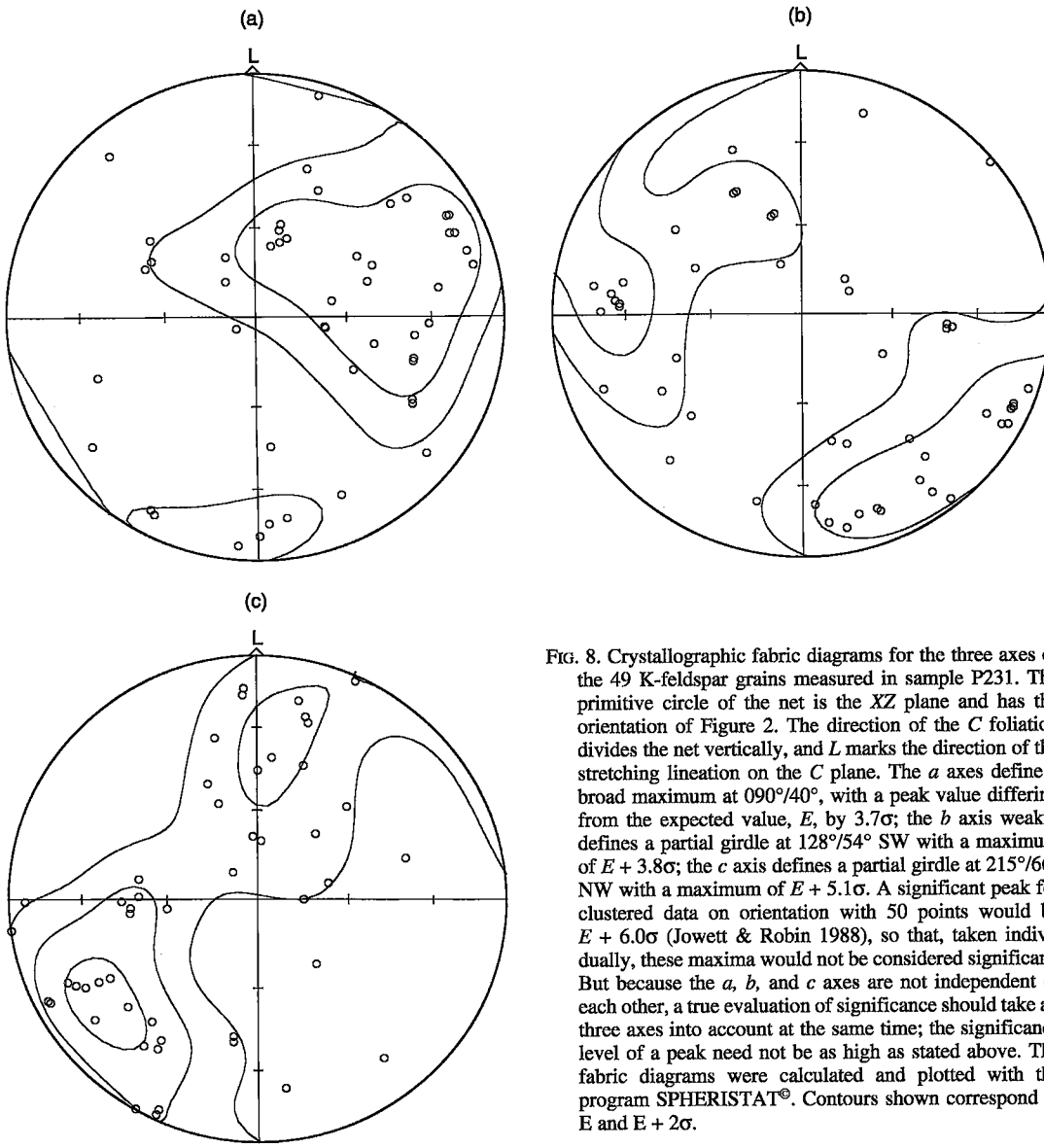

FIG. 8. Crystallographic fabric diagrams for the three axes of the 49 K-feldspar grains measured in sample P231. The primitive circle of the net is the *XZ* plane and has the orientation of Figure 2. The direction of the *C* foliation divides the net vertically, and *L* marks the direction of the stretching lineation on the *C* plane. The *a* axes define a broad maximum at 090°/40°, with a peak value differing from the expected value, *E*, by 3.7σ; the *b* axis weakly defines a partial girdle at 128°/54° SW with a maximum of $E + 3.8\sigma$; the *c* axis defines a partial girdle at 215°/66° NW with a maximum of $E + 5.1\sigma$. A significant peak for clustered data on orientation with 50 points would be $E + 6.0\sigma$ (Jowett & Robin 1988), so that, taken individually, these maxima would not be considered significant. But because the *a*, *b*, and *c* axes are not independent of each other, a true evaluation of significance should take all three axes into account at the same time; the significance level of a peak need not be as high as stated above. The fabric diagrams were calculated and plotted with the program SPHERISTAT©. Contours shown correspond to E and $E + 2\sigma$.

Relative orientation of intergrowths

The similarity of the ECPs from the K-feldspar (Figs. 9a,c) and the albite (Figs. 9b, d) from individual grains is striking. In Figure 9, the difference is approximately 2° in both cases. The difference in orientation of crystallographic axes for 15 host–flame pairs ranges from 0 to 10°, with a mode of less than 5° (Table 1). Stereoplots of the *b* crystallographic axes of the 15 host–flame pairs (Fig. 10) show similar crystallographic orientations in each host–flame pair. Angular differences of the order of 5° are expected for two reasons: (1) repeatedly indexing the same pattern commonly yields differences of 2°, and (2) some differences between crystallographic directions in albite and microcline are expected owing to the differences of 0.5 to 3° in unit-cell angles. The crystallographic relationship between host and lamellae can thus be described as homotactic. The term *homotaxy* carries no genetic implications. If two sets of lamellae occur within a single K-feldspar host (Fig. 1c), homotaxy is observed in both sets (Fig. 10, grain 113).

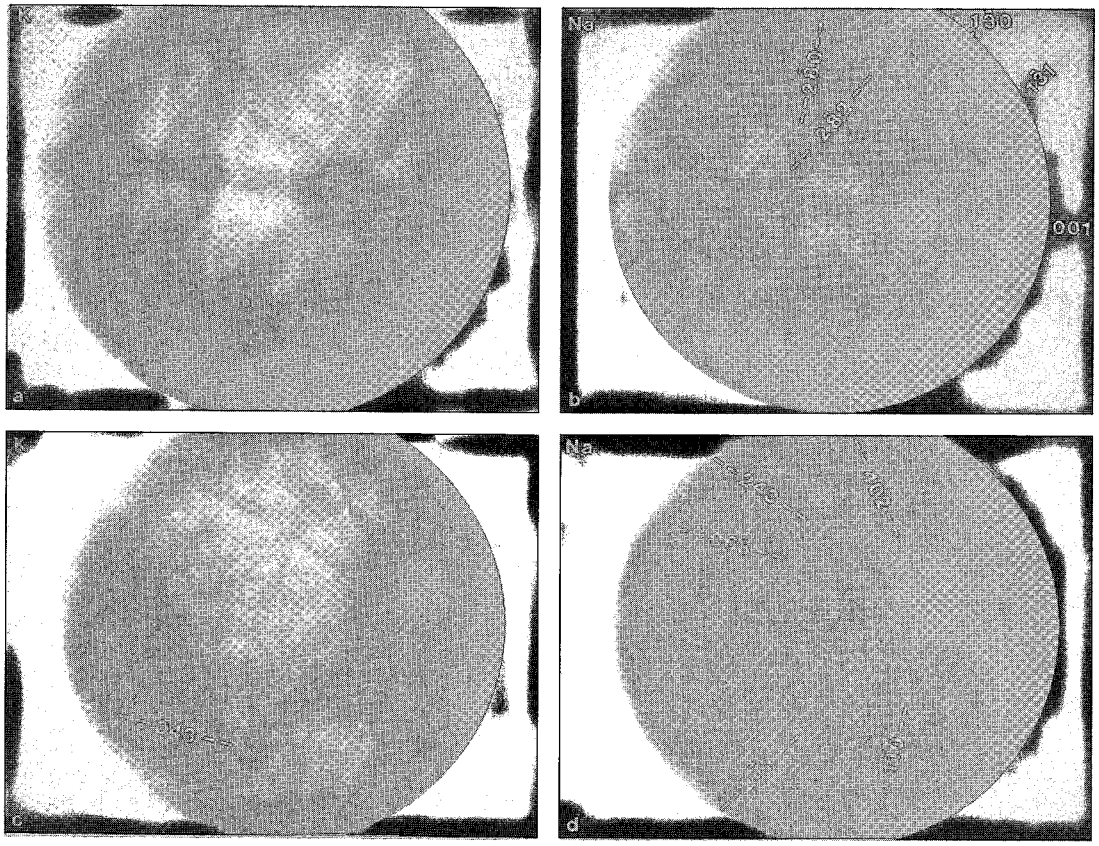

FIG. 9. ECPs of host–flame pairs showing very similar patterns with virtually identical orientations. (a),(b): P231, grain 111; (c),(d): P139, grain 005. Miller indices shown for the reflectors imaged in the ECP are the same for both K-feldspar and albite The curve in the (001) band of the K-feldspar pattern in (a) is a result of high-temperature deformation (hot-working).

TABLE 1. ANGULAR DIFFERENCES BETWEEN CRYSTALLOGRAPHIC AXES OF HOST-FLAME PAIRS

Sample	[100]	[010]	[001]
P139 001	5	5	3
002	7	7	8
003	5	1	5
004	2	6	6
005	6	7	2
P231 111	1	3	2
112	4	2	6
113	3	2	3
114	1	4	4
115	2	6	6
116	3	4	4
117	5	0	5
118	2	3	3
119	5	5	3
120	10	5	10
Average	4.1	4.6	4

Determination of crystallographic control of intergrowth interface

When working with rocks in section, it is never possible to determine the complete orientation of a planar feature; only the line of intersection between the plane of interest and the plane of the section, *i.e.*, the trace, can be determined accurately. To determine the plane of the flame–host interface within the K-feldspar, the trend of a flame trace in the BSE image of each perthite grain was measured relative to a reference axis (the edge of the photograph). The orientations of the traces measured were plotted as points on the perimeter of an equal-area net (Fig. 11); the perimeter of the net in this case represents the plane of the BSE image. The *a*, *b* and *c* axes of the host grain given by CHANNEL© also were plotted. The trend of the flame and the crystallographic axes of the host were rotated as linear elements to bring the *b* axis to the vertical position and then the *a* axis parallel to the right-hand side of the horizontal axis of the

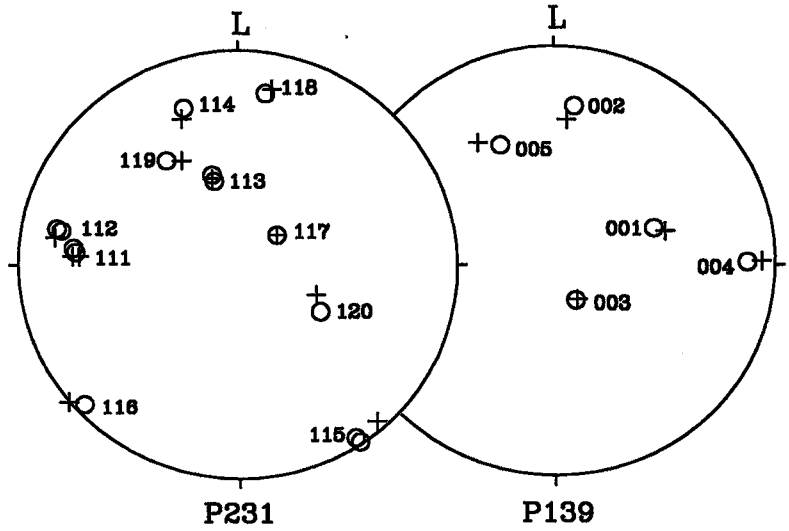

FIG. 10. Lower hemisphere, equal-area-net representation of the orientation of the *b* axes of all measured host–flame pairs. The orientation of the net is the same as in Figure 9. ○ : K-feldspar; + : Albite. Numbers adjacent to each pair of symbols are grain numbers. The maximum angular difference between host and flame is 5°.

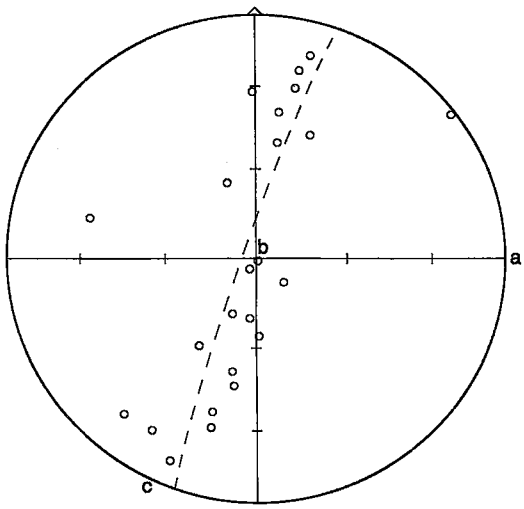

FIG. 11. Distribution of the flame traces on the plane of the section after rotation of crystallographic axes into coincidence. Flame trends, which are linear measurements, define a great circle parallel to the *b* axis and ~9° from the *c* axis, *i.e.*, the same orientation as normal perthite. The *b* axis is in the center of the stereonet; *a* and *c* are within 2.5° of the primitive circle in the directions shown. The dashed great circle represents the plane of the maximum and minimum eigenvectors calculated from the data points by SPHERISTAT, using the Jacobi method (*e.g.*, Cheeney 1983).

stereonet. This procedure was repeated on separate nets for each of the perthitic grains analyzed. Once all of the rotations were completed, all flame trends were traced onto one stereoplot (Fig. 11) to check for any consistency in orientation. The trends of the flame tips define a great circle approximately 9° from the *c* axis and parallel to the *b* axis, which corresponds closely to the orientation of the direction of minimum misfit between the structures of the two feldspar crystals in perthite (Smith 1961). In the few cases where more than one set of flames occur within a single grain, the trend of each set was measured, but there are not enough data to determine if a secondary preferred orientation exists, although some minor sets occur parallel to cleavage planes.

DISCUSSION

Orientation of flames relative to the rock fabric

The preferred orientation of the flames relative to the axes of finite strain in the host rock (Fig. 3) indicates that there is a control on the replacement process related to the orientation of grains within the structural frame of reference. As the flames also have a crystallographically controlled growth-plane, it therefore follows that the host K-feldspar must have a specific crystallographic orientation within the local stress-field in order to develop flames. Further discussion of this relationship and a detailed physical model for the

growth of albite flames are presented in Pryer (1993b) and Pryer & Robin (1992).

Relative orientation of host and lamellae

The preferred orientation of the flames within the K-feldspar crystal (Fig. 11) is the same as in "normal" perthite: parallel to the direction of minimum lattice misfit between the albite and K-feldspar structures predicted by both the "optimal" phase-boundary theory (Bollmann & Nissen 1968) and the coherency model, based on minimization of strain energy (*e.g.*, Robin 1974). Pryer & Robin (1992) argued that the growth of the albite occurs by replacement of K by Na without migration of Si, Al and O. The homotaxic relationship between these two feldspar phases suggests that the albite uses the existing Al–Si framework of the K-feldspar, and the homotaxic relationship can be specified as topotaxy. Pryer & Robin (1992) proposed a model in which coherent propagation of a flame tip results in the topotaxic relationship observed.

Origin of the preferred orientation of K-feldspar

The deformation of these rocks took place at mid-greenschist-grade conditions, well below the temperature necessary to significantly activate any slip systems in feldspars; the main mechanism of deformation in the feldspars is brittle fracture. Any nonrandom fabric must therefore result from a grain-shape fabric. The preferred orientation in the K-feldspar fabric diagrams (Fig. 8) must be related to the preferred orientation of fracture-fragments of feldspar within the mylonite, as feldspar fracturing is strongly dictated by the cleavage [(001) perfect, (010) good]. Fractures in sample P231 are strongly antithetic (Pryer 1993a, Fig. 6), oriented at 45° to the *C*-plane subparallel to the *S*-foliation. If the fabric were completely controlled by the (001) cleavage, the resulting *c*-axis fabric would be a small-circle distribution of 20° to 30° about a direction 45° from the *C*-plane, normal to the fracture-fragments. The maximum in the *c*-axis diagram (Fig. 8c) is in this position. As the orientations measured were not all derived from cleavage fragments, this alignment of fragments can only be partly responsible for the overall fabric. As pointed out earlier, these data may be biased by the indexing, and more data are required to allow further speculation on the crystallographic fabric of these rocks.

Problems with indexing feldspars

The success rate in indexing the feldspars in this study is low and should be discussed. Problems with the predicted ECPs remain. For example, with the structural parameters used here, some predicted band-intensities for third- and higher-order reflections are stronger than observed. Conversely, some bands are observed in the ECPs with a higher intensity than predicted. The possibility that the source of these discrepancies arises from the model of electron interactions used in CHANNEL is under investigation. However, these differences may be due to a number of causes that also plague other methods of structure determinations in feldspars. (1) The degree of order in the feldspars analyzed could be different from the degree of order assumed in the input file. In natural feldspars, particularly orthoclase, local and long-range variations in degree of order are common (*e.g.*, Smith 1974). (2) The effects on ECPs of submicrometric twinning, and consequent pseudomonoclinic symmetry (C2/*m*), in albite, and of twinning and tweed structures in K-feldspar are not known. Manifestations of these substructures may be either an average of the structure or a superposition of local ECPs.

Indexing is also affected by spatial variability in composition and degree of order. The pattern collected at one point in one grain may be different from that of another point, so that some ECPs are more exact matches to the predicted pattern.

In addition, the feldspars examined here are derived from mylonite zones, and are therefore expected to be deformed. The effect of cold working is a loss of sharpness in the ECP, which results in a difference in band widths. Hot working causes curved bands; as a result, the orientations chosen when digitizing the bands can vary by several degrees. ECPs from areas in which the crystal is obviously damaged are generally not indexable. But it is also possible for the damage to be such that a good pattern is obtained, yet is still sufficiently distorted to prevent indexing. The version of CHANNEL used here requires a precision in diffraction angles of minutes of degrees; subsequent versions require less precision and index much more quickly with no loss of accuracy.

Indexing the albite was a problem. Attempts to index the ECPs based on the parameters of Amelia low albite (Harlow & Brown 1980) were unsuccessful. Partial success was achieved with those of the synthetic high albite of Prewitt *et al.* (1976), in that some of the reflection bands were identified. But the exact position of the ECP along that band was located only after some manual searching of the ECP map. In our view, the slightly better results achieved with the high albite model do not imply that the albite flames are high albite. For one or more reasons, most likely submicrometric twinning, deformation, or chemical composition, the ECPs obtained were identified more readily by CHANNEL with the high albite model. It must be pointed out that once an ECP is identified, the pattern is unique and unambiquous. Whereas CHANNEL is confused by small differences in unit-cell parameters, an experienced operator could, with much patience, index albite with a microcline ECP map (see Fig. 9).

The problems with ECP analysis of feldspars are complex and beyond the scope of this study. Our aim

was to show the applicability of SEM–EC to a geological problem that could not be handled easily by any other single method, *i.e.*, to determine feldspar crystallographic orientations with micrometric resolution, without losing any spatial information. One possible way to address these problems is with preliminary analysis using the TEM. Electron-diffraction patterns provide cell dimensions specific to the area analyzed, that, along with X-ray chemical analysis, can be used to create the input file for the indexing software. The Kikuchi patterns obtained might then provide a test of the ECP model. TEM can also directly image twinning and dislocations and can therefore test the effect these have on the Kikuchi pattern.

Conclusions

SEM electron-channeling patterns can be used to determine the crystallographic orientation of perthite intergrowths while retaining spatial information. Indexed ECPs give both the relative orientations of the two phases and the crystallographic fabric in the host rock. The method is ideally suited for this type of work, (*i.e.*, orientation relationships of mineral intergrowths such as in flame perthite) and is the only single analytical method available from which all the orientation relationships desired can be determined on a large number of grains. However, the problems with indexing ECPs of feldspars need to be addressed before the SEM–EC can become a routine tool to study the feldspars.

Using SEM–ECPs, host–flame structures in flame perthite are found to be essentially topotaxic, suggesting that albite flames grow by direct Na-for-K replacement in a continuous Al–Si framework. Albite flames in K-feldspar are most often seen to grow along the "normal" perthite orientation, which is also the predicted orientation for minimum boundary-energy or for minimum elastic strain-energy between these two phases. Rarely, flames follow other orientations that may correspond to cleavage planes or fractures. The preferred orientation of the flames relative to the strain fabric in the host rock, combined with the preferred growth-plane within the K-feldspar structure, indicate that replacement occurs in those grains in which the plane for "normal" perthite is oriented parallel to the externally applied maximum principal stress.

Acknowledgements

We thank Joseph C. White, David Mainprice, Frank C. Hawthorne and Robert F. Martin for their careful reviews, which led to significant improvements to the manuscript. David Mainprice also provided the input files for feldspar indexing. Funding for this research was provided by grants of the Natural Sciences and Engineering Research Council of Canada to L.L.P. and P.-Y.F.R. and of the N.E.R.C. (U.K.) to G.E.L.

References

Berthé, D., Choukroune, P. & Jegouzo, P. (1979): Orthogneiss, mylonite and non coaxial deformation of granites: the South Amorican Shear-Zone. *J. Struct. Geol.* **1**, 31-42.

Blasi, A., Brajkovic, A. & De Pol Blasi, C. (1984): Dry-heating conversion of low microcline to high sanidine via a one-step disordering process. *Bull. Minéral.* **107**, 423-435.

Bollmann, W. & Nissen, H.-U. (1968): A study of optimal phase boundaries: the case of exsolved alkali feldspars. *Acta Crystallogr.* **A24**, 546-557.

Cheeney, R.F. (1983): *Statistical Methods in Geology for Field and Lab Decisions*. Allen & Unwin, London, U.K.

Coates, D.G. (1967): Kikuchi-like reflection patterns obtained with the scanning electron microscope. *Philos. Mag., 8th ser.*, **16**, 1179-1184.

Haggart, M.J., Jamieson, R.A., Reynolds, P.H., Krogh, T.E., Beaumont, C. & Culshaw, N.G. (1993): Last gasp of the Grenville Orogeny: thermochronology of the Grenville Front Tectonic Zone near Killarney, Ontario. *J. Geol.* **101**, 575-589.

Harlow, G.E. & Brown, G.E. (1980): Low albite: an x-ray and neutron diffraction study. *Am. Mineral.* **65**, 986-995.

Jowett, E.C. & Robin, P.-Y.F. (1988): Statistical significance of clustered orientation data on the sphere: an empirical derivation. *J. Geol.* **96**, 591-599.

Joy, D.C., Newbury, D.E. & Davidson, D.L. (1982): Electron channeling patterns in the scanning electron microscope. *J. Appl. Phys.* **53**, R88-R122.

Lister, G.S. & Snoke, A.W. (1984): S–C mylonites. *J. Struct. Geol.* **6**, 617-638.

Lloyd, G.E. (1985): Review of instrumentation, techniques and applications of SEM in mineralogy. *In* Applications of Electron Microscopy in the Earth Sciences (J.C. White, ed.). *Mineral. Assoc. Can., Short-Course Handbook* **11**, 151-188.

_____ (1987): Atomic number and crystallographic contrast images with the SEM: a review of backscattered electron techniques. *Mineral. Mag.* **51**, 3-19.

_____ & Ferguson, C.C. (1986): A sperical electron-channeling pattern map for use in quartz petrofabric analysis. *J. Struct. Geol.* **8**, 517-526.

_____, Hall, M.G., Cockayne, B. & Jones, D.W. (1981): Selected-area electron-channeling patterns from geological materials: specimen preparation, indexing and representation of patterns and applications. *Can. Mineral.* **19**, 505-518.

Newbury, D.E., Joy, D.C., Echlin, P., Fiori, C.E. & Goldstein, J.I. 1986. *Advanced Scanning Electron Microscopy and X-Ray Microanalysis*. Plenum Press, New York, N.Y.

PREWITT, C.T., SUENO, S. & PAPIKE, J.J. (1976): The crystal structures of high albite and monalbite at high temperatures. *Am. Mineral.* **61**, 1213-1225.

PRYER, L.L. (1993a): Microstructures in feldspars from a major crustal thrust zone: the Grenville Front, Ontario, Canada. *J. Struct. Geol.* **15**, 21-36.

_____ (1993b): *A Model for the Origin of Flame Perthite: the Roles of Retrograde Metamorphism and Differential Stress.* Ph.D. dissertation, Univ. Toronto, Toronto, Ontario.

_____ & ROBIN, P.-Y.F. (1992): A stress induced replacement model for the origin of flame perthite. *Geol. Soc. Am., Abstr. Program* **24**(7), A322.

ROBIN, P.-Y.F. (1974): Stress and strain in cryptoperthite lamellae and the coherent solvus of alkali feldspars. *Am. Mineral.* **59**, 1299-1318.

SCHMIDT, N.-H. & OLESEN, N.Ø. (1989): Computer-aided determination of crystal-lattice orientation from electron-channeling patterns in the SEM. *Can. Mineral.* **27**, 15-22.

SMITH, J.V. (1961): Explanation of strain and orientation effects in perthites. *Am. Mineral.* **46**, 1489-1493.

_____ (1974): *Feldspar Minerals.* **1.** *Crystal Structure and Physical Properties.* Springer-Verlag, Berlin, Germany.

Received July 16, 1993, revised manuscript accepted April 19, 1994.